References and Notes

1. J. A. Davies, *Bioessays* **24**, 937 (2002).
2. R. J. Metzger, M. A. Krasnow, *Science* **284**, 1635 (1999).
3. B. L. Hogan, P. A. Kolodziej, *Nat. Rev. Genet.* **3**, 513 (2002).
4. M. M. Zegers, L. E. O'Brien, W. Yu, A. Datta, K. E. Mostov, *Trends Cell Biol.* **13**, 169 (2003).
5. J. Que, M. Choi, J. W. Ziel, J. Klingensmith, B. L. Hogan, *Differentiation* **74**, 422 (2006).
6. J. E. Fata, Z. Werb, M. J. Bissell, *Breast Cancer Res.* **6**, 1 (2004).
7. R. B. Widelitz, J. M. Veltmaat, J. A. Mayer, J. Foley, C. M. Chuong, *Semin. Cell Dev. Biol.* **18**, 255 (2007).
8. M. M. Shah, R. V. Sampogna, H. Sakurai, K. T. Bush, S. K. Nigam, *Development* **131**, 1449 (2004).
9. V. N. Patel, I. T. Rebustini, M. P. Hoffman, *Differentiation* **74**, 349 (2006).
10. G. R. Dressler, *Annu. Rev. Cell Dev. Biol.* **22**, 509 (2006).
11. W. V. Cardoso, J. Lü, *Development* **133**, 1611 (2006).
12. B. S. Spooner, H. A. Thompson-Pletscher, B. Stokes, K. E. Bassett, *Dev. Biol.* **3**, 225 (1986).
13. T. Sakai, M. Larsen, K. M. Yamada, *Nature* **423**, 876 (2003).
14. S. E. Gill, M. C. Pape, K. J. Leco, *Dev. Biol.* **298**, 540 (2006).
15. S. P. De Langhe *et al.*, *Dev. Biol.* **277**, 316 (2005).
16. M. Larsen, C. Wei, K. M. Yamada, *J. Cell Sci.* **119**, 3376 (2006).
17. C. Grobstein, *Nature* **172**, 869 (1953).
18. W. P. Daley, K. M. Gulfo, S. J. Sequeira, M. Larsen, *Dev. Biol.* **336**, 169 (2009).
19. J. L. Walker *et al.*, *Dev. Dyn.* **237**, 3128 (2008).
20. S. Zollman, D. Godt, G. G. Privé, J. L. Couderc, F. A. Laski, *Proc. Natl. Acad. Sci. U.S.A.* **91**, 10717 (1994).
21. R. Perez-Torrado, D. Yamada, P. A. Defossez, *Bioessays* **28**, 1194 (2006).
22. F. Martin-Belmonte, K. Mostov, *Curr. Opin. Cell Biol.* **20**, 227 (2008).
23. M. Gossen, H. Bujard, *Proc. Natl. Acad. Sci. U.S.A.* **89**, 5547 (1992).
24. P. Leroy, K. E. Mostov, *Mol. Biol. Cell* **18**, 1943 (2007).
25. J. Roman, *Exp. Lung Res.* **23**, 147 (1997).
26. We thank M. Hoffman, M. Larsen, and K. Musselmann for advice. T.O. was supported by a fellowship from the Japan Society for the Promotion of Science (JSPS). This work was supported in part by the Intramural Research Program of the NIH, NIDCR, and by Grants-in-Aid for Scientific Research (B) (21390534) from the JSPS to T.S. The SAGE data sets are available at the Gene Expression Omnibus (GEO) database under accession number GSE22374.

Early Chordate Origins of the Vertebrate Second Heart Field

Alberto Stolfi,[1] T. Blair Gainous,[1] John J. Young,[1] Alessandro Mori,[1]*
Michael Levine,[1]† Lionel Christiaen[1,2]†

The vertebrate heart is formed from diverse embryonic territories, including the first and second heart fields. The second heart field (SHF) gives rise to the right ventricle and outflow tract, yet its evolutionary origins are unclear. We found that heart progenitor cells of the simple chordate *Ciona intestinalis* also generate precursors of the atrial siphon muscles (ASMs). These precursors express *Islet* and *Tbx1/10*, evocative of the splanchnic mesoderm that produces the lower jaw muscles and SHF of vertebrates. Evidence is presented that the transcription factor COE is a critical determinant of ASM fate. We propose that the last common ancestor of tunicates and vertebrates possessed multipotent cardiopharyngeal muscle precursors, and that their reallocation might have contributed to the emergence of the SHF.

The vertebrate heart initially forms as a tube from a population of precursor cells termed the first heart field (FHF). Cells from the adjacent second heart field (SHF) are then progressively added to the developing heart (*1*, *2*). In avian and mammalian hearts, the FHF contributes mainly to the left ventricle, whereas the SHF gives rise to the outflow tract and large portions of the right ventricle and atria. Both fields arise from common mesodermal progenitors, although the detailed lineage relationships between FHF and SHF remain uncertain (*1*, *3*). SHF-like territories have been identified in frog (*4*, *5*), zebrafish (*6*), and lamprey (*7*), yet evidence for a deeper evolutionary origin remains obscured by the absence of a clear SHF in invertebrates (*8*).

Tunicates are the sister group to the vertebrates (*9*). Studies on a model tunicate, the ascidian *Ciona intestinalis*, have revealed conserved regulatory mechanisms underlying chordate heart de-velopment (*10*). The *Ciona* heart arises from a pair of blastomeres (named the B7.5 cells, by Conklin's nomenclature) in gastrulating embryos (*11*). Localized expression of *MesP* in B7.5 cells determines their competence to form the heart (Fig. 1A) (*12*, *13*). Subsequently, fibroblast growth factor signaling induces expression of *FoxF* and the heart determinants *NK4* (*tinman/Nkx2.5*), *GATAa*, and *Hand-like/NoTrlc* in the anterior B7.5 granddaughter cells [the trunk ventral cells (TVCs)] (Fig. 1B) (*13*, *14*). FoxF activates downstream target genes that control the migration of the TVCs to the ventral trunk region (Fig. 1C) (*14*, *15*).

After metamorphosis, descendants of the B7.5 lineage give rise to the heart (Fig. 1D). B7.5 de-scendants also generate the atrial siphon muscles (ASMs) that surround the excurrent openings of the peribranchial atrium (Fig. 1D), as well as lon-gitudinal muscles (LoMs) arising from the ASMs during metamorphosis (fig. S7). The contribution of the B7.5 lineage to ASMs is consistent with conventional lineage tracing performed in the dis-tantly related ascidian *Halocynthia roretzi* (*16*). Cardiomyocytes and ASMs are distinguished by expression of the myosin heavy chain (MHC) genes *MHC2* and *MHC3* (*17*), respectively (fig. S3). Thus, they constitute distinct muscle types arising from common progenitor cells.

Live imaging of the B7.5 lineage cells allowed the characterization of events leading to the sepa-ration of heart and ASMs (Fig. 1E). After their migration to the ventral trunk region, each TVC undergoes two successive asymmetric divisions along the mediolateral axis to produce six cells on either side of the ventral midline (Fig. 1, E and F, time points 0 to 2; movie S1). The larger daughter cells (lateral TVCs) are positioned lateral to the smaller medial TVCs. Subsequent symmetric cell divisions result in an array of ~24 cells: eight lateral TVCs (four on either side) bracketing 16 medial TVCs (Fig. 1, E and F, time points 3 to 5; movie S2) (*18*).

A second migration occurs several hours after hatching. Each group of lateral TVCs detaches from the medial TVCs and migrates dorsally as a polarized cluster of cells on either side of the trunk. They eventually form a ring of cells under-neath the atrial siphon primordia (Fig. 1, G and H, and movie S3). Targeted inhibition of TVC specification blocked the formation of ASMs (fig. S4). These observations demonstrate that the lateral TVCs correspond to the precursors of the ASMs.

The ASMs are evocative of vertebrate jaw muscles arising from lateral/splanchnic meso-derm (SpM): *Ciona* TVCs and vertebrate anterior SpM both express orthologs of *Nkx2.5* and *FoxF* and derive from progenitors that expressed *MesP* during gastrulation (*5*, *19*, *20*). In chick and mouse embryos, much of the anterior SpM gives rise to the SHF, but some precursors migrate into the first branchial arch and form intermandibular muscles (*21*, *22*). A key marker of the anterior SpM and SHF is the LIM-homeodomain transcription fac-tor Islet1 (Isl1) (*4–6*, *21*). The single *Ciona Islet* (*23*) gene is expressed in several tissues including the ASM precursors, which maintain *Islet* expres-sion during their migration away from the medial TVCs (fig. S1). The latter possibly show weak and transient *Islet* expression, which is reminiscent of that reported in the FHF of vertebrates (*19*).

Islet expression was further characterized using defined enhancers (fig. S2). Reporter trans-genes containing ~3.2 kb of the *Islet* 5′ flanking region exhibited localized expression in the lat-eral TVCs, and in ASMs in juveniles (Fig. 2, A to C). In contrast, *MesP* reporter transgenes labeled the entire B7.5 lineage, including both ASMs and heart (e.g., Fig. 1, C and D, and fig. S5). The

[1]Center for Integrative Genomics, Division of Genetics, Ge-nomics and Development, Department of Molecular and Cell Biology, University of California, Berkeley, CA 94720, USA. [2]Center for Developmental Genetics, Department of Biology, New York University, 1009 Silver Center, 100 Washington Square East, New York, NY 10003, USA.

*Present address: Forest Laboratories Inc., 909 Third Avenue, New York, NY 10022, USA.

†To whom correspondence should be addressed. E-mail: mlevine@berkeley.edu (M.L.); lc121@nyu.edu (L.C.)

Fig. 1. Contribution of trunk ventral cells (TVCs) to heart and atrial siphon muscles (ASMs). (**A**) Immuno-detection of β-gal expression (green) in B7.5 cells in a gastrulating embryo transfected with *MesP>lacZ* transgene. (**B**) Visualization of *MesP>lacZ* (green) and *FoxF[TVC enhancer]>mCherry* (red) expression in B7.5 descendants in a tailbud-stage embryo. (**C**) Expression of a *MesP>Histone2B(H2B)::GFP* fusion protein (green) in a tadpole. (**D**) Visualization of *MesP>H2B::CFP* (green) in a stage 38 juvenile [~100 hours post-fertilization (hpf)]. Expression is visible in the heart (arrowhead), ASMs, and longitudinal muscles (LoMs) (arrows). *MesP* is activated only in the B7.5 pair of cells at the gastrula stage. a.s., atrial siphon; o.s., oral siphon. (**E**) Frames from movie S1 (time points 0 to 2) and S2 (time points 3 to 5). Dashed line indicates ventral midline. Right-side cells are partially visible at time points 1 and 2. Stereotyped cell divisions (see text) result in four lateral TVCs on either side of the embryo flanking ~16 medial TVCs. The four lateral TVCs on either side detach and migrate to form ASMs. Medial cells form the heart. Cells were visualized as two independent time-lapse sequences of embryos transfected with *MesP>H2B::GFP/CFP*. (**F**) Cartoon representing the events in (E). (**G** and **H**) Frames from movie S3 showing left-side ASM precursors expressing *MesP>H2B::mCherry* (red) and *MesP>PH::GFP* (green). ASM precursors encircle the siphon primordium, between 21 hpf (G) and 23 hpf (H). Scale bars, 50 μm [(A) to (D)], 20 μm (E). Asterisks identify anterior tail muscles (ATMs).
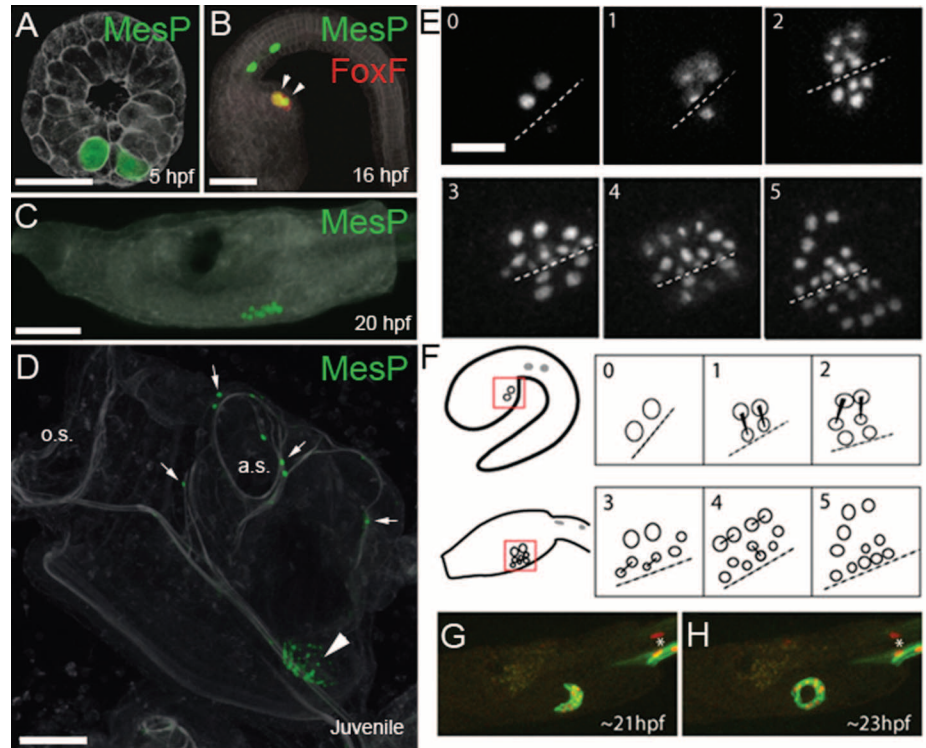

Fig. 2. ASM-specific gene expression. (**A**) Dorsal view of electroporated larva exhibiting mosaic incorporation (left side) of *Islet>GFP* (green) and *MesP>H2B::mCherry* (red) transgenes at 20 hpf, before the migration of the lateral TVCs. *Islet>GFP* expression is restricted to lateral TVCs. Dotted line indicates midline; M and L indicate medial and lateral, respectively. (**B**) Lateral view of larva expressing same transgenes as in (A) at 24 hours, after migration of *Islet>GFP*-positive lateral TVC descendants around the atrial siphon primordium. D, dorsal; V, ventral. (**C**) Juvenile (~100 hpf) raised from embryo transfected with *Islet>H2B::mCherry* (red), with transgene expression visible around atrial siphons (arrow) and longitudinal muscles (arrowheads), but not heart (Ht). F-actin is stained by phallacidin (blue-green). Scale bar, 100 μm. (**D**) Magnified view (see fig. S7) of LoMs (arrowhead) segregating from ASMs (arrows) during metamorphosis, visualized by *MesP>lacZ* expression (red). Panel width is ~100 μm. (**E**) In situ hybridization of *Tbx1/10* (green). (**F**) Merged view of (D) and (E), showing activation of *Tbx1/10* in LoMs. (**G**) *COE* expression in lateral TVCs at 20 hpf revealed by in situ hybridization. Dotted line indicates ventral midline.
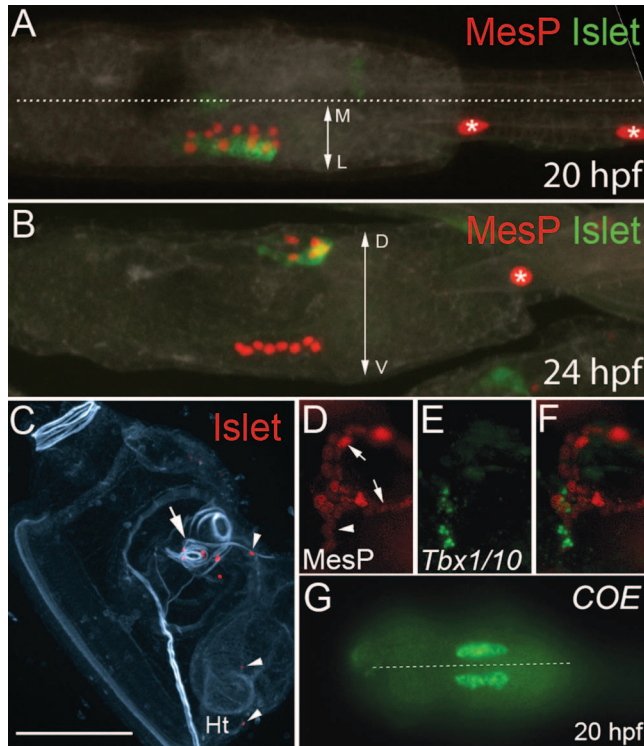
heart primordium is situated ventrally and medi-ally to the *Islet⁺* ASM progenitors (Fig. 2A). This is reminiscent of the positioning of the FHF rel-ative to *Isl1⁺* SHF/pharyngeal mesoderm in basal vertebrates (*4*, *5*, *7*). Furthermore, LoM precursors segregating from the ASMs express the *Ciona* ortholog of *Tbx1* (*24*), an important regulator of SHF and pharyngeal mesoderm development in vertebrates (*25*) (Fig. 2, D to F, and fig. S7). Taken together, these results suggest homology between the ASM/LoM precursors of tunicates and the progenitors of lower jaw muscles and SHF of vertebrates.

Preliminary functional assays suggest that Is-let is not instructive for the specification of ASMs (fig. S10). In the course of these studies, we found that the transcription factor *Collier/Olf1/EBF* (*COE*) is expressed early in the ASM precursors (Fig. 2G and fig. S11). To determine whether this localized expression is instructive for ASM specification, we used the *FoxF* TVC enhancer to misexpress COE in all TVCs (*13*). In 96% of transfected embryos, all TVC descendants mi-grated toward the atrial siphon placodes and ex-pressed *Islet>GFP* (Fig. 3, A and B, fig. S6, and movie S4). More than half (56%) of the trans-fected embryos grew into juveniles that lacked a heart but still had ASMs (Fig. 3, D, E, and G to J, and fig. S6), which suggests that COE is suf-ficient to specify a lateral TVC identity and sub-sequent ASM fate.

Similar misexpression of a repressor form of COE (COE::WRPW) resulted in the reciprocal phenotype: All TVC descendants remained in the ventral trunk, and *Islet>GFP* expression was abolished (Fig. 3, A and C, and fig. S6). Upon metamorphosis, TVC descendants differentiated into enlarged hearts (Fig. 3, D, F to H, K, and L, and fig. S8). Inhibition of COE function thus trans-forms the entire TVC lineage into heart tissue, in-

Fig. 3. COE controls ASM specification. (**A** to **C**) Larvae cotransfected with *MesP>H2B::mCherry* (red), *Islet>GFP* (green), and (A) *FoxF>lacZ*, (B) *FoxF>COE*, or (C) *FoxF>COE::WRPW*. (B) All TVCs are transformed into ASM precursors (arrows). No heart primordium is formed (dashed triangle). (C) All TVC descendants form a heart (arrowhead) with no *Islet>GFP* expression. (**D**) Juveniles raised from embryos transfected with *MesP>H2B::mCherry* (red), counterstained with phallacidin (blue-green). H2B::mCherry[+] B7.5 descendants populate the heart (Ht) and ASMs (arrows) (residual larval muscle staining indicated by asterisk). (**E**) Cotransfection with the *FoxF>COE* transgene, resulting in no heart (usual location indicated by dashed circle) but normal ASMs (arrow). (**F**) Coexpression of the *FoxF>COE:WRPW* transgene. TVCs form an expanded heart and there are no ASMs (arrow). (**G** and **H**) In situ hybridization on wild-type juveniles, showing *MHC3* and *MHC2* expression in ASMs (arrow) and heart, respectively. (**I** and **J**) *FoxF>COE* results in loss of *MHC2* expression (dashed circle), but not *MHC3* expression (arrow). (**K** and **L**) *FoxF>COE::WRPW* abolishes *MHC3* expression (arrow) and leads to expanded *MHC2* expression. Scale bars, 50 μm; o.s., oral siphons.
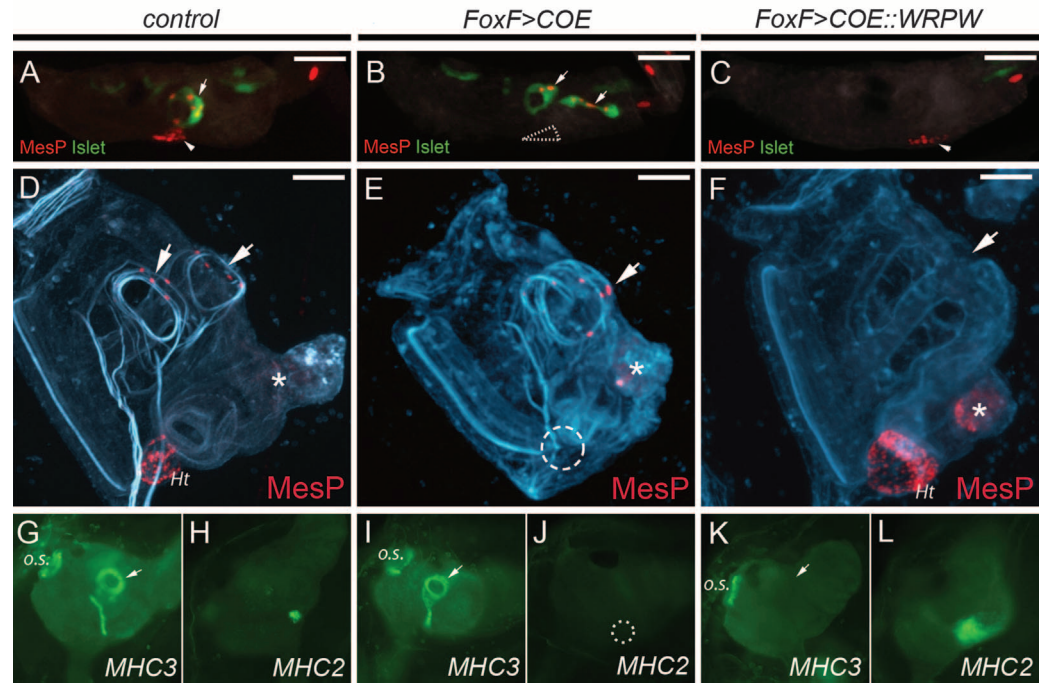
Fig. 4. Comparison to vertebrate pharyngeal mesoderm. (**A** to **C**) Expression of the *COE* ortholog *Xebf2* and anterior lateral mesoderm/SHF markers *Nkx2.5* and *Islet1* in *X. tropicalis* embryos at NF stage 20. (A) Expression of *Xebf2* (white arrow) partially overlaps that of *Islet1* (B) and *Nkx2.5* (C) in pharyngeal mesoderm lateral to the heart primordium. Scale bar, 500 μm. (**D** and **E**) The cardiopharyngeal lineages of *Ciona* (D) and vertebrates (E). (D) Summary of differential expression of selected regulatory genes in the B7.5 lineage. (E) Expression of orthologous genes in mouse development. Evolutionary reallocation of *Islet1*^{+} cardiopharyngeal precursors toward the heart might have given rise to the SHF.
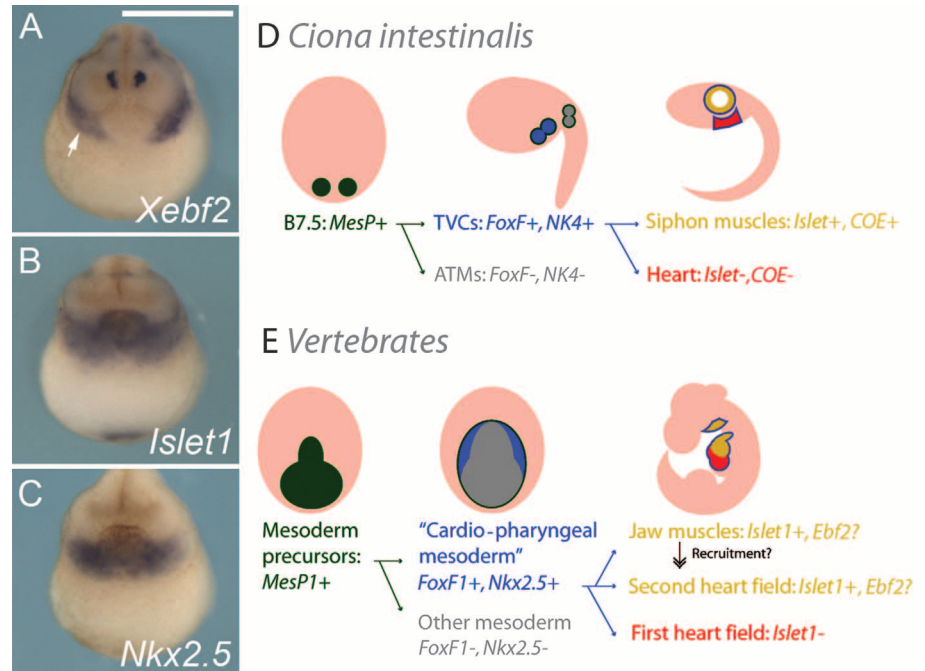
dicating that COE activity is required for ASM specification.

The COE homolog Collier/Knot is involved in muscle type specification in *Drosophila* (26), but a role for COE in vertebrate SHF or jaw muscle development has not been reported. As a first step toward determining whether COE factors might play a conserved role in vertebrates, we performed in situ hybridization of the *COE* orthologs *Xebf2* and *Xebf3* in *Xenopus tropicalis* embryos (Fig. 4, A to C, and fig. S9). *Xebf2* ex-

pression was seen in *Nkx2.5*[+]/*Isl1*^{+} anterior lateral mesoderm, where *Tbx1* is also expressed (5).

The preceding results suggest that the last common ancestor of tunicates and vertebrates had a population of cardiopharyngeal mesoderm, which (i) arose from *MesP*-expressing early mesoderm, (ii) expressed orthologs of *FoxF* and *Nkx2.5*, and (iii) had the potential to give rise to both heart tissue and pharyngeal muscles, which (iv) correlated with differential maintenance of *Islet* expression. Moreover, *COE* might be a con-

served determinant of chordate pharyngeal mesoderm development.

We propose that the reallocation of *Islet*[+] cardiopharyngeal progenitors among the heart and cranial myogenic fields supported the emergence of the SHF (Fig. 4, D and E). In *Ciona*, *Islet*^{+} cells do not contribute to the heart, but targeted expression of COE::WRPW was sufficient to convert them into cardiomyocytes. It is conceivable that the reallocation of *Islet*[+] pharyngeal muscle progenitors toward SHF depended on the interca-

lation of cardiac regulatory network components (e.g., *GATA4*, *Mef2c*) downstream of *Islet* (*27*).

An ancient connection between heart and craniofacial muscles has been proposed on the basis of the role of an *Nkx2.5* ortholog in the pharynx of the nematode *Caenorhabditis elegans*, which lacks a heart (*28*). *Haikouella lanceolata*, a fossil chordate from the Lower Cambrian, shows a putative heart adjacent to a muscularized pharyngeal atrium (*29*). The shared lineage of cardiomyocytes and pharyngeal muscles in tunicates hints that a pool of common precursors could have formed both heart and pharyngeal atrium muscles in a *Haikouella*-like ancestor. Northcutt and Gans (*30*) proposed that muscular ventilation of the pharyngeal arches was a key transition in the evolution of the vertebrates. Therefore, the cardiopharyngeal mesoderm could have been instrumental in the coevolution of circulatory, respiratory, and feeding functions in tunicates and vertebrates.

References and Notes

1. M. Buckingham, S. Meilhac, S. Zaffran, *Nat. Rev. Genet.* **6**, 826 (2005).
2. R. Abu-Issa, M. L. Kirby, *Annu. Rev. Cell Dev. Biol.* **23**, 45 (2007).
3. S. M. Meilhac, M. Esner, R. G. Kelly, J. F. Nicolas, M. E. Buckingham, *Dev. Cell* **6**, 685 (2004).
4. T. Brade, S. Gessert, M. Kühl, P. Pandur, *Dev. Biol.* **311**, 297 (2007).
5. S. Gessert, M. Kuhl, *Dev. Biol.* **334**, 395 (2009).
6. E. de Pater et al., *Development* **136**, 1633 (2009).
7. N. Kokubo et al., *Evol. Dev.* **12**, 34 (2010).
8. J. M. Perez-Pomares, J. M. Gonzalez-Rosa, R. Munoz-Chapuli, *Int. J. Dev. Biol.* **53**, 1427 (2009).
9. F. Delsuc, H. Brinkmann, D. Chourrout, H. Philippe, *Nature* **439**, 965 (2006).
10. B. Davidson, *Semin. Cell Dev. Biol.* **18**, 16 (2007).
11. Y. Satou, K. S. Imai, N. Satoh, *Development* **131**, 2533 (2004).
12. L. Christiaen, A. Stolfi, B. Davidson, M. Levine, *Dev. Biol.* **328**, 552 (2009).
13. B. Davidson, W. Shi, J. Beh, L. Christiaen, M. Levine, *Genes Dev.* **20**, 2728 (2006).
14. J. Beh, W. Shi, M. Levine, B. Davidson, L. Christiaen, *Development* **134**, 3297 (2007).
15. L. Christiaen et al., *Science* **320**, 1349 (2008).
16. T. Hirano, H. Nishida, *Dev. Biol.* **192**, 199 (1997).
17. M. Ogasawara et al., *Dev. Genes Evol.* **212**, 173 (2002).
18. B. Davidson, W. Shi, M. Levine, *Development* **132**, 4811 (2005).
19. O. W. Prall et al., *Cell* **128**, 947 (2007).
20. J. Kang, E. Nathan, S. M. Xu, E. Tzahor, B. L. Black, *Dev. Biol.* **334**, 513 (2009).
21. E. Nathan et al., *Development* **135**, 647 (2008).
22. E. Tzahor, *Dev. Biol.* **327**, 273 (2009).
23. P. Giuliano, R. Marino, M. R. Pinto, R. De Santis, *Mech. Dev.* **78**, 199 (1998).
24. N. Takatori et al., *Dev. Dyn.* **230**, 743 (2004).
25. Z. Zhang, T. Huynh, A. Baldini, *Development* **133**, 3587 (2006).
26. M. Crozatier, A. Vincent, *Development* **126**, 1495 (1999).
27. E. N. Olson, *Science* **313**, 1922 (2006).
28. P. G. Okkema, E. Ha, C. Haun, W. Chen, A. Fire, *Development* **124**, 3965 (1997).
29. J. Y. Chen, D. Y. Huang, C. W. Li, *Nature* **402**, 518 (1999).
30. C. Gans, R. G. Northcutt, *Science* **220**, 268 (1983).
31. We thank D. Hendrix for computational analysis, A. Cooc for technical assistance, and R. Harland, I. Philipp, and T. J. Park for advice. Supported by NSF grant IOB 0445470 (M.L.), NIH training grant 0745322 (T.B.G.), and a New York University Faculty of Arts and Science start-up package (L.C.).

Identification of a Cell of Origin for Human Prostate Cancer

Andrew S. Goldstein,[1] Jiaoti Huang,[2,3,6] Changyong Guo,[2,4] Isla P. Garraway,[2,4] Owen N. Witte[1,5,6]*

Luminal cells are believed to be the cells of origin for human prostate cancer, because the disease is characterized by luminal cell expansion and the absence of basal cells. Yet functional studies addressing the origin of human prostate cancer have not previously been reported because of a lack of relevant in vivo human models. Here we show that basal cells from primary benign human prostate tissue can initiate prostate cancer in immunodeficient mice. The cooperative effects of AKT, ERG, and androgen receptor in basal cells recapitulated the histological and molecular features of human prostate cancer, with loss of basal cells and expansion of luminal cells expressing prostate-specific antigen and alpha-methylacyl-CoA racemase. Our results demonstrate that histological characterization of cancers does not necessarily correlate with the cellular origins of the disease.

Prostate cancer research has been hindered by an absence of model systems in which the disease is initiated from primary human prostate epithelial cells, precluding investigation of transforming alterations and cells of origin. Commonly used human prostate cancer cell lines and xenografts are derived from metastatic lesions. Murine prostate cancer models prohibit testing of species-specific therapies such as monoclonal antibodies against human proteins (*1*). An ideal model system would be human cell–derived and present as a multifocal disease, to accurately represent the heterogeneity of prostate malignancy (*2*). The system should allow one to investigate the role that specific genetic alterations and paracrine signals play in disease initiation and progression. Finally, the model system should be highly malleable, allowing for comparisons of lesions derived from different cell populations or driven by different genetic alterations. We created such a system by directly transforming naïve adult human prostate epithelium with genetic alterations that are commonly found in human prostate cancer. Activation of the PI 3-kinase pathway, typically via loss of PTEN (*3*), and increased expression of the

ETS-family transcription factor ERG through chromosomal translocation (*4*) occur frequently together in human prostate cancer and cooperate to promote disease progression in mice (*5–7*). Androgen receptor (AR) is commonly up-regulated in human prostate cancer, and the androgen signaling axis is implicated in late-stage disease (*8*).

Luminal cells are generally accepted as the cells of origin for human prostate cancer (*9*, *10*), because pathologists diagnose the disease based on the absence of basal cell markers (*11*). Evidence from the mouse implicates both luminal cells (*12–14*) and basal cells (*15–17*) in prostate cancer initiation. Although murine cancer cell-of-origin studies typically involve transgenic mice with oncogene expression or Cre-mediated deletion of tumor suppressors driven by cell type–specific promoters (*18*), parallel studies in the human system require both a method to reliably separate subpopulations of primary cells and an in vivo transformation model.

In addition to rare neuroendocrine cells and reported intermediate phenotypes, the three main epithelial cell populations described in the human prostate are K5 (keratin 5)$^+$ K14$^+$ K8/18^{lo} basal cells, K5$^+$ K14$^-$ K8/18^{lo} basal cells, and K5$^-$ K14$^-$ K8/18^{hi} luminal cells (*19*). No commonly accepted strategy exists to isolate such populations from dissociated human prostate tissue. We have previously demonstrated expression of CD49f (integrin alpha 6) and Trop2 (TACSTD2) in human prostate tissue by immunohistochemical staining and flow cytometry, where these two antigens distinguish four separate populations (*20*, *21*). To determine the cellular identities of each population, we performed intracellular flow cytometry for basal (K14) and luminal (K18) keratins on primary human prostate cells, in addition to Western blot and quan-

[1]Molecular Biology Institute, University of California, Los Angeles (UCLA), Los Angeles, CA 90095, USA. [2]Jonsson Comprehensive Cancer Center, UCLA, Los Angeles, CA 90095, USA. [3]Department of Pathology and Laboratory Medicine, UCLA, Los Angeles, CA 90095, USA. [4]Department of Urology, UCLA, Los Angeles, CA 90095, USA. [5]Department of Microbiology, Immunology and Molecular Genetics; Department of Molecular and Medical Pharmacology; Howard Hughes Medical Institute, David Geffen School of Medicine, UCLA, Los Angeles, CA 90095, USA. [6]Eli and Edythe Broad Center of Regenerative Medicine and Stem Cell Research, UCLA, Los Angeles, CA 90095, USA.

*To whom correspondence should be addressed at Howard Hughes Medical Institute, UCLA, Los Angeles, 675 Charles E. Young Drive South, 5-748 MRL, Los Angeles, CA 90095–1662, USA. E-mail: owenwitte@mednet.ucla.edu

Science

Early Chordate Origins of the Vertebrate Second Heart Field

Alberto Stolfi, T. Blair Gainous, John J. Young, Alessandro Mori, Michael Levine and Lionel Christiaen

Building the Heart

The multichambered heart of birds and mammals develops through addition of second heart field (SHF)–derived precursor cells to a primary heart tube. **Stolfi** *et al.* (p. 565) show that, in the simple chordate *Ciona intestinalis*, the heart and atrial siphon muscle (ASM) precursors arise from common progenitors following asymmetric cell divisions and that the transcription factor COE (Collier/Olf1/EBF) is involved in this fate choice. The ASM precursors express molecular markers of the vertebrate pharyngeal mesoderm that gives rise to the SHF and lower jaw muscles, suggesting that the origins of both can be traced back to the last common ancestor of tunicates and vertebrates.

ARTICLE TOOLS	http://science.sciencemag.org/content/329/5991/565
SUPPLEMENTARY MATERIALS	http://science.sciencemag.org/content/suppl/2010/07/29/329.5991.565.DC1
REFERENCES	This article cites 30 articles, 12 of which you can access for free http://science.sciencemag.org/content/329/5991/565#BIBL
PERMISSIONS	http://www.sciencemag.org/help/reprints-and-permissions

Use of this article is subject to the Terms of Service